applied sciences

MDPI

Article

Phytochemical Constituents and Biological Properties of Finger Lime (*Citrus australasica* F. Muell.) Peel, Pulp and Seeds

Daniela De Vita [1], Anna Rita Stringaro [2], Marisa Colone [2], Maria Luisa Dupuis [2], Fabio Sciubba [1,3], Luigi Scipione [4] and Stefania Garzoli [4,*]

[1] Dipartimento di Biologia Ambientale, Università di Roma "La Sapienza", Piazzale Aldo Moro 5, 00185 Rome, Italy; daniela.devita@uniroma1.it (D.D.V.); fabio.sciubba@uniroma1.it (F.S.)
[2] National Center for Drug Research and Evaluation, Italian National Institute of Health, 00161 Rome, Italy; annarita.stringaro@iss.it (A.R.S.); marisa.colone@iss.it (M.C.); marialuisa.dupuis@iss.it (M.L.D.)
[3] NMR-Based Metabolomics Laboratory (NMLab), Università di Roma "La Sapienza", Piazzale Aldo Moro 5, 00185 Rome, Italy
[4] Department of Chemistry and Technologies of Drug, Sapienza University, Piazzale Aldo Moro 5, 00185 Rome, Italy; luigi.scipione@uniroma1.it
* Correspondence: stefania.garzoli@uniroma1.it

Abstract: In this work, for the first time, different parts of the Finger Lime (*Citrus australasica* F. Muell.), such as pulp, peel and seeds, were analyzed by HS-SPME-GC/MS, and NMR techniques in order to describe its volatile and non-volatile chemical profile. The results highlighted the presence of a high number of terpenes with limonene as principal component in all investigated parts (ranging from 40.4% to 62.6%) and molecules belonging to the classes of amino acids, organic acids, carbohydrates, fatty acids, phenols and miscellaneous compounds that followed a different trend between the investigated different parts. In this study, the inhibition of ChEs (AChE and BChE) was evaluated using the spectrophotometric method of Ellman. The results showed that only peel extract weakly inhibited AChE (14%). Based on these data, this extract was further investigated by GC/MS after derivatization. Furthermore, peel extract was chosen to evaluate the in vitro effects on two human glioblastoma cells lines (U87 and LN18). Flow cytometry results showed that citrus extract was more effective in down-regulating the expression of the adhesion molecule CD44. In fact, after 72 h with 400 µg/mL of citrus extract, CD44 expression levels were reduced in both U87 and LN18 glioblastoma cell lines. This was confirmed by immunofluorescence analysis, which also showed a modification of CD44 antigen localization in both U87 and LN18 cell lines. Moreover, wound assay data supported its ability to reduce glioblastoma cell's motility. The migration ability of U87 cells decreased (85% control vs. 50% at 400 µg/mL), while it was even more pronounced in resistant LN18 cells (93% control vs. 15% at 400 µg/mL). The findings highlighted that citrus peel extract could have an anti-invasive activity for glioma management.

Keywords: caviar lime; chemical analyses; biological activity; motility inhibition; cell lines

Citation: De Vita, D.; Stringaro, A.R.; Colone, M.; Dupuis, M.L.; Sciubba, F.; Scipione, L.; Garzoli, S. Phytochemical Constituents and Biological Properties of Finger Lime (*Citrus australasica* F. Muell.) Peel, Pulp and Seeds. *Appl. Sci.* **2024**, *14*, 6498. https://doi.org/10.3390/app14156498

Academic Editors: Ivona Elez Garofulić and Maja Repajić

Received: 29 June 2024
Revised: 20 July 2024
Accepted: 22 July 2024
Published: 25 July 2024

1. Introduction

Over time it has been demonstrated that regular fruit consumption is closely correlated with a lower risk of developing chronic diseases linked to oxidative stress thanks to the beneficial properties conferred by its bioactive fruit constituents [1]. Citrus fruits belonging to the *Citrus* L. genus (Rutaceae family) contain so many phytoconstituents belonging to different chemical classes that they are considered functional foods with multiple activities including antioxidant, anti-inflammatory and anticancer effects [2–4].

Citrus fruits are generally consumed fresh, but they are also used to produce jams, juices and more. During the manufacturing process, the peels are the main by-products which could represent a source of environmental pollution if unused. For this reason, in recent years there has been an attempt to valorize these by-products since, for various

fruits, they represent the main source of antioxidants and therefore can be used as natural preservatives [5].

Citrus australasica F. Muell., also known as "Finger lime", is a species native to Australia where it grows spontaneously thanks to the sub-tropical climate [6]. The plant can reach 6 m in height; it is thorny with small leaves and branches that tend to grow horizontally. The flowering period is spring, but in warm climates it can also continue into autumn. The flowers are small and white and give life to cylindrical green fruits which turn yellow when ripe [7]. It has very rich fruiting and its fruits are characterized by a rough skin and a pulp made up of tiny grains similar to pearls that vary from white to yellow or from pink to orange. These fruits are also filled with a liquid with an acidic flavor similar to that of lemon but sweeter. These pearls or round granules are very similar to caviar which is why the fruit is also called "vegetable caviar" or "caviar lime".

Over time, much work has been performed to develop new cultivars that differ in the color of the peel and pulp and the aroma [8]. Certainly, these differences are linked to a different chemical profile. Despite this, only in the last ten years has this species aroused considerable interest in the food sector. In fact, thanks to its scent and its particular shape, it is widely used by chefs to garnish fish or meat dishes [7].

To date, among all the species belonging to the *Citrus* genus, finger lime is under-investigated [9]. In line with the growing demand for health-promoting natural products, several analytical approaches are used to detect and describe the presence of bioactive phytochemical constituents in foods.

Therefore, in the present study, to provide more compositional and functional information about the Finger lime, a metabolomic approach based on gas chromatography/mass spectrometry (GC/MS) and nuclear magnetic resonance (NMR) was performed, to characterize the peel, pulp and seeds of the Finger lime grown in Switzerland. In order to increase knowledge on the potential bioactivities of this fruit, an evaluation of the inhibition of ChEs (AChE and BChE) by the spectrophotometric method was performed on the three different parts of the fruit. Furthermore, the peel extract has been subjected to wound testing and is considered to evaluate in vitro effects on two human glioblastoma cell lines (U87 and LN18).

2. Materials and Methods

2.1. Plant Materials

A *C. australasica* sample (Figure 1), the object of this study, was grown in the Nyon region, Switzerland and supplied by Niels Rodin's citrus farm. A ripe fruit, weighing approximately 8 g, was harvested in October 2020 and stored in a fridge (about 5 °C) until analysis. Before use, it was washed with deionized water and the mesocarp was manually separated from the exocarp.

Figure 1. Illustration of *Citrus australsica* fruit.

2.2. SPME-GC/MS Analysis of Peel, Pulp and Seeds

Chemical volatile composition of the untreated *C. australasica* was investigated by SPME-GC/MS technique. To this aim, thin slices of peel, pulp and seeds, approximately 2 g each, were individually placed into a 7 mL glass vial with PTFE-coated silicone septum. The sampling was performed by SPME technique [10,11]. To capture the volatiles, a

SPME device from Supelco (Bellefonte, PA, USA) with 1 cm fiber coated with 50/30 µm DVB/CAR/PDMS (divinylbenzene/carboxen/polydimethylsiloxane) was used. The fiber was initially conditioned and then exposed to the headspace of the samples for 20 min at 40 °C. Once the sampling phase was completed, the fiber was inserted into the GC injector kept at 250 °C for the desorption of the captured analytes.

A Clarus 500 model Perkin Elmer (Waltham, MA, USA) gas chromatograph coupled with a mass spectrometer and equipped with a FID (flame detector ionization) was used to perform the analyses. In detail, a Varian Factor Four VF-1 capillary column was housed in the GC oven. The temperature ramp was set as follows: 40 °C for 2 min, then increasing to 220 °C at 6/min, and finally held for 10 min. Helium was the carrier gas at flow rate of 1.0 mL min^{-1} in splitless mode. MS apparatus was equipped with an electron impact ionization (EI) that operated at 70 eV in scan mode in the range 35–450 m/z. The identification of components was carried out by matching their mass spectra with those stored in the Nist 11 mass spectra library database and by comparison of the calculated linear retention indices (LRIs), relative to C_8–C_{30} *n*-alkanes, with those reported in the literature. The amounts of the identified molecules were expressed as percentage of the relative peak area, obtained from the FID signal to that of the total peak area. No internal standard or factor correction was used. All analyses were carried out in triplicate.

2.3. Extraction Procedures

The samples were treated with EtOH 96% v/v with a ratio matrix/solvent of 1 g:10 mL and macerated for 24 h at room temperature. The extraction was repeated 3 times. The ethanolic solutions were reunited and evaporated under vacuum at 40 °C. The obtained dry extract was used for subsequent analyses.

2.4. GC-MS Analysis of the Peel Extract after Derivatization

To describe the chemical composition of the non-volatile portion of the peel, a derivatization reaction was performed on the extract. For this purpose, approximately 2 mg of the dried extract was added to 250 µL of pyridine and 80 µL of *bis*-(trimethylsilyl) trifluoroacetamide (BSTFA) with heating at 80 °C for 30 min. To perform the analysis the same apparatus GC-FID/GC-MS and the same capillary column (Varian Factor Four VF-1), were used. A total of 2 µL of the silylated extract was injected at 280 °C into the GC injector in the splitless mode. The temperature conditions applied were as follows: 60 °C, then a gradient of 7 °C/min to 170 °C for 1.0 min, a gradient of 7 °C/min to 250 °C, and a gradient of 8 °C/min to 300 °C for 25 min. For the identification of the compounds, the percentage of similarity and the comparison of the mass spectra (MS) relating to each individual peak with those of the NIST software (version 1.1) data library, were considered. For the quantification, relative percentages were obtained by electronic integration of the GC-FID peak areas, and no response factors were calculated.

2.5. NMR Analysis of the Peel, Pulp and Seeds

C. australasica was also analyzed by NMR spectroscopy. In particular, a non-polar, a semi-polar and a polar fraction were examined for each portion of the fruit. The non-polar fractions were resuspended in 700 µL of $CDCl_3$, the semi-polar in 700 µL of DMSO and the polar 700 µL of D_2O containing 3-(trimethylsilyl)-2,2,3,3-d4-propionate sodium (TSP) as chemical shift reference. The spectra were acquired on a JNM-ECZ 600R spectrometer, equipped with a 14.09 Tesla magnet with an operating frequency for hydrogen of 600 MHz and a multinuclear head. The one-dimensional spectra were acquired with a given number of points equal to 64 k, a spectral amplitude of 15 ppm (corresponding to 9000 Hz), 128 scans and a recycle time of 7.7 s for a total of 15 s per scan to guarantee the complete relaxation of the resonances.

The molecules in the spectra were identified on the basis of their chemical shift, multiplicity and a comparison with the literature data [12].

2.6. Inhibition of Cholinesterases (ChEs)

To evaluate the inhibition of ChEs (AChE and BChE), the spectrophotometric method of Ellman with minor modifications [13], was used. AChE (Electric eel AChE, EC 3.1.1.7), BChE (equine serum BChE, 3.1.1.8) acetylthiocholine iodide (ASCh), butyrylthiocholine iodide (BSCh) and 5,5′-dithio-*bis*-(2-nitrobenzoic acid) (DTNB) were purchased from Sigma-Aldrich (Milan, Italy). The assay was performed by a double beam UV-Vis lambda 40 Perkin Elmer spectrophotometer, using optical polystyrene cuvettes (10 10 45 mm, 340–800 nm optical transparency). Each extract was dissolved in methanol/water (70:30 v/v) in the opportune quantity in order to obtain a final cuvette organic solvent content that does not affect the enzyme activity (<0.1%). Peel and pulp were diluted to a concentration of 100 mg mL^{-1}, while seeds were diluted to 25 mg mL^{-1}.

Percent Inhibition of ChE

A total of 3.0 mL of 0.1 M (pH 7.4) phosphate buffer containing DTNB (0.25 mM) and ChE (0.083 U mL^{-1}) were placed in a polystyrene cuvette of 1.0 cm path length; 1 µL of a solution of the tested extract was added. Then, 30 µL of a 10 mM aqueous solution in phosphate buffer (pH = 7.4) of ASCh or BSCh was added to achieve a final concentration of 100 µM of substrate. The increasing amount of the yellow 5-nitro-2-tio benzoic anion (λmax 412 nm), produced by the enzymatic hydrolysis of the substrate, was recorded at 25 °C between 0.5 and 1.5 min. The control without inhibitor, corresponding to 100% of the enzymatic activity, was prepared in the same way. Each experiment was repeated in triplicate. The percent inhibition was calculated using the following equation:

$$\text{inhibition } (\%) = \frac{A_c - A_i}{A_c} \times 100$$

where A_i and A_c represent the change in the absorbance in the presence of inhibitor and without inhibitor, respectively.

2.7. Cells Cultures

U-87 (U-87 HTB-14TM) and LN18 (CRL-2610) cell lines from the human brain (glioblastoma astrocytoma) (ATCC, Manassas, VA, USA) LN18 [14,15], were grown in DMEM/F12 (Euroclone) supplemented with 10% FBS (Corning South America, Sial) at 37 °C in a humidified atmosphere containing 5% CO_2 and subcultured before confluence using 0.05% trypsin and 0.002% EDTA solution.

2.8. Cell Viability Assay

Cell viability was evaluated using an MTT assay. Briefly, glioma cells were seeded into 96-well microtiter plates (Nunclon TM, Nunc, Germany) at a density of 8×10^4 cells/well. After 24 h cells were treated with the peel extract at concentration of 0.5, 1, 5, 10, 20, 40, 80, 100, 150, 200 and 400 µg/mL. After an incubation time of 48 h, the medium was replaced by a fresh one containing 0.5 mg/mL of MTT (Sigma, Deisenhofen, Germany). After an incubation time of 2 h at 37 °C, unreacted dye was removed, and the purple formazan product was dissolved in 200 µL/well of dimethylsulfoxide (Merck, Darmstadt, Germany) and absorbance was read at 570 nm by a Microplate Spectrophotometer (Thermo Scientific Multiskan SkyHigh, Carlsbad, CA, USA). The data were expressed as absorbance relative to untreated cells in the same experiment and standardized to 100%. All data points were performed in triplicate. Results are the average of three independent experiments.

2.9. Cell Cycle Analysis

U-87 and LN18 cells were seeded in complete medium (3×10^5/25 cm^2 flask). After 24 h, they were treated with 100, 200 and 400 µg/mL for 24, 48 and 72 h at 37 °C. Then, both floating and adherent cells were collected, washed twice with cold PBS and centrifuged. The pellet was fixed in 70% ethanol in distilled water at 4 °C for 1 h, washed twice with cold PBS and then resuspended in PBS containing 40 µg/mL propidium iodide (PI) and

100 μg/mL RNAse, at 37 °C for 1 h. Samples were then analyzed by a flow cytometry instrument (Gallios Instrument, Beckman Coulter, Brea, CA, USA). After activation of the "doublet discrimination module" and exclusion of cell debris defining a gate in the side and forward scatter dot-plot, at least 10,000 events per sample were acquired in linear mode. The percentages of cells in the different phases were analyzed using Kaluza software for analysis v. 2.2 (Beckman Coulter).

2.10. Wound Assay

Cells were added and allowed to adhere to the culture plate in 24-well plates 2.5×10^5 (cell number was matched across conditions within each given experiment). A total of 24 h later, cells were treated with peel extract (100 and 200 and 400 μg/mL) and immediately scratched using a 200 μL sterile pipette tip. After 24 h of treatment, cells were fixed using 70% ice-cold ethanol and then were stained by Crystal violet dye and observed using an inverted microscope equipped with an Olympus camera. Wound areas were measured using the select tool in ImageJ software (version 1.54j). The calculated areas were then statistically compared using SPSS software (version 29.0).

2.11. CD44 Expression by Flow Cytometric Analysis

The level of CD44 positivity was evaluated using a flow cytometer. Cells (1×10^6) were cultured in 25 cm 2 flasks and treated with 100, 200 and 400 μg/mL of the peel extract for 48 and 72 h. After treatment, cells were collected and then incubated for 1 h with anti-mouse monoclonal CD44 antibody (2 μg/mL in Phosphate buffer saline, PBS) (HCAM Antibody DF1485-Santa Cruz Biotechnology, Inc. Bergheimer, Heidelberg, Germany). For negative controls, cells were incubated with mouse IgG1 isotype immunoglobulins at a concentration of 2 μg/mL in PBS. The samples were then washed with ice-cold PBS containing 10 mM NaN_3 and 1% BSA (Sigma) and incubated for 30 min at 4 °C with a secondary goat anti-mouse IgG Alexa-Fluor 488-conjugate (Invitrogen, Eugene, OR, USA) at 1:50 dilution. After two washes in cold PBS, the cells were labeled with propidium iodide (PI, Sigma, final concentration 40 μg/mL) and immediately analyzed by a flow cytometry instrument (Gallios). Fluorescence emissions were collected through 530 nm and 570 nm band-pass filters for Alexa-Fluor and PI signals, respectively. At least 10.000 cells per sample were acquired in log mode, and only PI-negative cells were considered for analysis. The data were analyzed using Kaluza software (version 2.2), (Beckman Coulter, Milan, Italy) and expressed as mean ± standard deviation from three independent experiments.

2.12. CD44 Expression by Immunofluorescence Microscopy Observations

Glioma cells were grown on coverslips and treated with the peel extract at 200 and 400 μg/mL for 48 h. Then, cells were fixed with 4% *p*-formaldehyde in phosphate-buffered saline (PBS, pH 7.4) for 30 min at room temperature. After washing in the same buffer, samples were permeabilized with 0.5% Triton X-100 (Sigma Chemicals Co., St. Louis, MO, USA) in PBS for 5 min at room temperature. To detect CD44, cells were stained with the anti-mouse monoclonal CD44 antibody HCAM Antibody (2 μg/mL) for 1 h, followed by incubation with the goat anti-mouse IgG Alexa-Fluor 488-conjugate secondary antibody (Invitrogen™, Eugene, OR, USA, 1:100 work solution). Then, cells were washed with PBS containing 10 mM NaN_3 and 1% BSA and incubated for 30 min at 37 °C with the dye Alexa Fluor™ Plus 555 Phalloidin (Invitrogen™) to detect F-actin (filamentous actin). The cells were finally stained with Hoechst 33258 (861405, Sigma-Aldrich, St Louis, MO, USA, 1:10.000 work solution) for nuclei detection at 37 °C for 15 min. After a final PBS wash, coverslips were mounted using a 2:1 mixture of glycerol and phosphate-buffered saline and images were acquired using a Ti2 Nikon ECLIPSE microscope (Florence, Italy).

2.13. Statistical Analysis

Data were expressed as means ± SD of three individual experiments; statistical significance was determined by unpaired *t*-test, considering *p*-values < 0.05 statistically significant, according to GraphPad Prism 10.

3. Results and Discussion

3.1. Volatile Chemical Composition

SPME-GC/MS analysis allowed to describe the volatile fraction from the headspace of fresh *C. australasica* peel, pulp and seeds. In total, eighteen compounds have been identified and are listed in Table 1.

Table 1. Chemical composition (percentage mean value ± standard deviation) of *C. australasica* peel, pulp and seeds.

N°	COMPONENT [1]	LRI [2]	LRI [3]	Peel [4] (%)	Pulp [5] (%)	Seeds [6] (%)
1	α-thujene	918	923	0.4 ± 0.02	0.4 ± 0.03	0.6 ± 0.03
2	α-pinene	935	943	1.5 ± 0.02	-	-
3	sabinene	958	962	-	0.8 ± 0.03	-
4	β-pinene	981	986	32.4 ± 0.15	-	-
5	α-phellandrene	1000	1005	-	0.5 ± 0.02	-
6	α-terpinene	1017	1019	0.2 ± 0.02	-	4.8 ± 0.05
7	limonene	1024	1023	62.6 ± 0.17	41.5 ± 0.20	40.4 ± 0.14
8	*cis*-β-ocimene	1035	1032	0.2 ± 0.02	0.4 ± 0.02	-
9	γ-terpinene	1049	1054	0.7 ± 0.03	14.8 ± 0.09	13.9 ± 0.07
10	isoterpinolene	1078	1081	0.1 ± 0.00	2.0 ± 0.02	1.3 ± 0.02
11	*trans*-sabinene hydrate	1091	1098	0.1 ± 0.02	38.4 ± 0.20	35.9 ± 0.11
12	1,3,8-*p*-menthatriene	1115	1118	-	0.7 ± 0.20	-
13	δ-elemene	1341	1347	0.6 ± 0.06	-	-
14	α-cubebene	1355	1350	0.1 ± 0.00	-	-
15	γ-elemene	1447	1445	1.0 ± 0.03	-	-
16	α-farnesene	1489	1496	-	0.2 ± 0.01	-
17	guaia-1(10),11-diene	1501	1505	-	0.3 ± 0.02	3.0 ± 0.03
	SUM			99.9	100.0	99.9
	Monoterpene hydrocarbons			98.1	60.4	61.0
	Oxygenated monoterpenes			0.1	38.4	35.9
	Sesquiterpene hydrocarbons			1.7	0.5	3.0
	Others			-	0.7	-

[1] the components are reported according to their elution order on apolar column; [2] linear retention indices measured on apolar column; [3] linear retention indices from the literature; peel [4]: percentage mean values of peel components (%); pulp [5]: percentage mean values of pulp components; seeds [6]: percentage mean values of seeds components—not detected; tr: traces (mean value < 0.1%). The analyses were conducted in triplicate.

In all three samples the monoterpene content exceeds the sesquiterpene one with limonene as the main compound reaching a percentage mean value of 62.6% in the peel, 41.5% in the pulp and 40.4% in the seeds. These data are in agreement with what was previously reported. In fact, limonene was found to be the main volatile constituent present in *C. australasica* peels although with percentage values that may vary compared to the total volatile content [7,16]. Relevant differences were detected between the investigated samples. From a qualitative point of view, the seeds were characterized by a fewer number of components detected. As known, VOCs compounds such as monoterpenes, sesquiterpenes and their oxygenated derivatives are primarily concentrated in the peel portion of the citrus fruit; in fact, essential oils are generally extracted from the peel. In contrast, the seeds are enriched in fixed oils sugars, tocopherols, phytosterols, carotenoids and minerals [17–19]. In the present work, β-pinene was detected only in the peel and with a significant relative

concentration (32.4%). Other components such as, sabinene (0.8%), α-phellandrene (0.5%), 1,3,8-*p*-menthatriene (0.8%) and α-farnesene (0.2%), were present only in the pulp. On the other hand, the sesquiterpenes δ-elemene (0.6%), α-cubebene (0.1%) and γ-elemene (1.0%) were found only in the peel. Elemene has been found to reverse drug resistance and sensitize cancer cells to chemotherapy. Possible mechanisms of action include the induction of apoptosis and autophagy and the regulation of the expression of key genes and proteins in various signaling pathways [20].

Trans-sabinene hydrate was mainly present in the pulp (38.4%) and in the seeds (35.9%) and was barely detected in the peel (0.1%). The pulp and seeds, however, contained a comparable relative percentage of γ-terpinene (14.8% and 13.9%).

3.2. Peel Extract Chemical Composition

By direct injection analyses of the silylated extract, a large number of compounds belonging to different chemical classes have been identified (Table 2). Carboxylic acids represented the most representative class of compounds both numerically and quantitatively. In fact, citric acid covered 88.7% of the total. This component has been reported to be the most abundant among carboxylic acids also by Ramón Aznar et al. [21]. Citric acid is a known antioxidant that acts to inhibit the oxidation of other molecules by scavenging reactive oxygen species (ROS) that are produced as by-products of normal cellular function [22]. Furthermore, clinical studies have shown how its antioxidant power can be useful for combating various disorders including metabolic, neurological (Alzheimer's disease) and cardiological disorders [23]. Both fatty acids and sugars were characterized by three components each whose relative percentages were less than 1%. The presence of the triterpene ursolic acid is interesting.

Table 2. Chemical composition (percentage values) of peel extract after derivatization.

N°	Component	Extract (%) [1]
	Carboxylic Acids	
1	pyruvic acid	tr
2	succinic acid	tr
3	itaconic acid	0.6
4	glycolic acid	0.2
5	malic acid	2.3
6	citric acid	88.7
7	quininic acid	2.8
8	ascorbic acid	0.2
	Fatty Acids	
9	linoleic acid	0.5
10	palmitic acid	0.5
11	*trans*-9-octadecenoic acid	0.9
	Sugars	
12	D-talopyranose	0.6
13	D-talofuranose	0.5
14	D-allofuranose	0.4
	Triterpenes	
15	ursolic acid	1.1

[1] Percentage values of the components of peel extract after derivatization. The analyses were conducted in duplicate.

3.3. NMR Results

In the examined samples it was possible to identify molecules belonging to the classes of amino acids, organic acids, carbohydrates, fatty acids, phenolics and miscellaneous compounds (Table 3). In all fruit parts, it was possible to detect the presence of amino

acids (valine, isoleucine, leucine, threonine, alanine, aspartate, asparagine, proline, tyrosine, phenylalanine and tryptophan), organic acids (citrate, malate and formate), carbohydrates: (sucrose, fructose and glucose), fatty acids: (stearate, oleate, linoleate and linolenate) and the alcohol ethanol.

Table 3. Qualitative Chemical composition assessed by NMR Spectroscopy.

Molecule		Peel	Pulp	Seed
Amino Acids	Valine	X	X	X
	Isoleucine	X	X	X
	Leucine	X	X	X
	Threonine	X	X	X
	Alanine	X	X	X
	Aspartate	X	X	X
	Asparagine	X	X	X
	Proline	X	X	X
	Tyrosine	X	X	X
	Phenylalanine	X	X	X
	Tryptophan	X	X	X
Organic Acids	Citrate	X	X	X
	Malate	X	X	X
	Formate	X	X	X
	4-hydroxycoumarate		X	X
	4-hydroxybenzoate		X	X
	Gallate		X	
Carbohydrates	Sucrose	X	X	X
	Fructose	X	X	X
	Glucose	X	X	X
Fatty Acids	Stearate	X	X	X
	Oleate	X	X	X
	Linoleate	X	X	X
	Linolenate	X	X	X
Other Compounds	Ethanol	X	X	X
	Quercetin-3-*O*-glycoside		X	X
	Trigonelline		X	X
	1,3,4-tryhydroxybenzene		X	
	Monoterpenes	X		
	Diterpenes	X		

In the pulp and seeds polar extracts only, it was possible to observe the presence of quinic acid, 4-hydroxycoumaric acid, 4-hydroxy benzoic acid, trigonelline and quercetin-3-*O*-glycoside; while in the pulp polar fraction only, it was possible to detect the presence of gallic acid and 1,3,4-trihydroxybenzene.

In the peel non-polar extract only, it was possible to identify mono- and diterpenes.

The analyses were conducted in duplicate.

3.4. Enzyme Inhibition

The extracts were evaluated as AChE and BChE inhibitors. As shown by the results in Table 4, only the peel weakly inhibits the enzyme. Some compounds identified in the extracts have shown cholinesterase inhibition. Sadaoui et al. [24], demonstrated that limonene, the main volatile terpene in *C. australasica,* inhibits AChE and BChE with an IC_{50} value of 51.6 ± 0.7 and 66.7 ± 12.6 μg mL^{-1}, respectively. The capacity to inhibit ChEs was found also for *β*-pinene [25], quercetin-3-*O*-glycoside [26] and ursolic acid [27]. Taking into consideration the phytochemical composition of *C. australasica*, the extracts were evaluated as AChE and BChE inhibitors. As shown by the results reported in Table 4, only the peel weakly inhibited the enzyme.

Table 4. Inhibition of cholinesterases by tested extracts.

Extract	AChE Inhibition (%)	BChE Inhibition (%)
Peel (33 μg mL^{-1}) [a]	14	NI
Pulp (33 μg mL^{-1}) [a]	NI	NI
Seeds (8 μg mL^{-1}) [a]	NI	NI

[a] Final concentration in cuvette, NI = no inhibition; the analyses were conducted in duplicate.

3.5. Cell Viability Assay

The possible cytotoxic activity of the citrus extract on the U87 and LN18 glioma cell lines was evaluated by MTT assay at 48 h with different concentrations (0.5, 1, 5, 10, 20, 40, 80, 100, 150, 200, and 400 μg/mL). The MTT assay results demonstrated that the citrus extract did not exhibit cytotoxic effects on U87 or LN18 glioma cell lines across the tested concentration range (0.5 to 400 μg/mL). In fact, the viability of U87 cells treated with citrus peel extract at concentrations ranging from 0.5 to 400 μg/mL remained above 70%, indicating non-cytotoxicity (Figure 2). Similarly, the viability of LN18 cells treated with the citrus extract at the same concentration range remained above 90%, confirming the non-cytotoxicity (Figure 3). These findings suggest that the citrus peel extract was safe for these cell lines at the tested concentrations and time point (Figure 3).

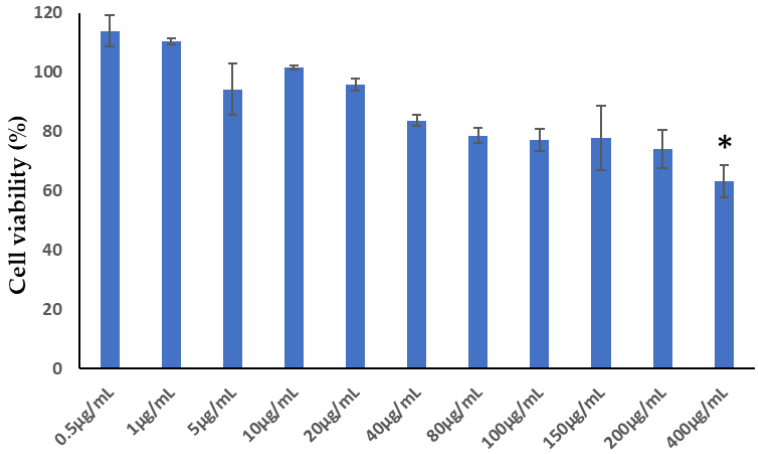

Figure 2. Cell viability analysis in U87 cells treated with peel extract at 48 h. All experiments were conducted in triplicate and the results are expressed as mean ± SD values. According to GraphPad Prism10, unpaired *t*-test, * *p*-value < 0.05.

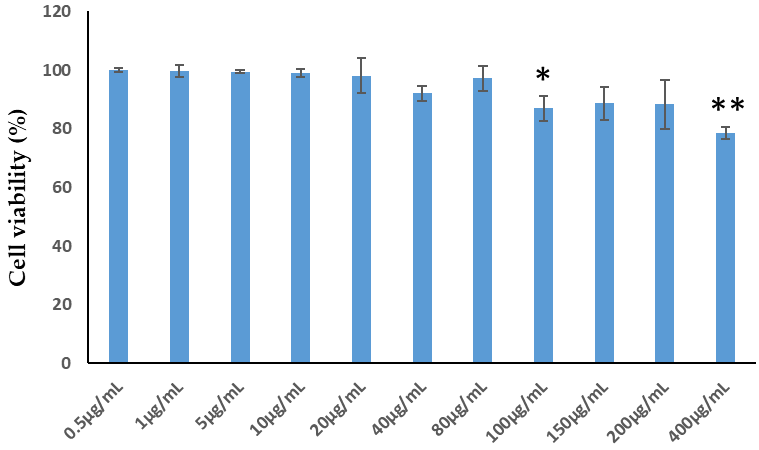

Figure 3. Cell viability analysis in LN18 cells treated with peel extract at 48 h. All experiments were conducted in triplicate and the results are expressed as mean ± SD values. According to GraphPad Prism10, unpaired *t*-test, * *p*-value < 0.05, ** *p*-value 0.01.

3.6. Cell Cycle Analysis

Cell cycle analysis was performed to gain further insights into the mechanism of the minimum effect of the phytocompound on cell viability. U87 and LN18 cells were treated for 24, 48, and 72 h with peel extract at concentrations of 100, 200, and 400 µg/mL. Flow cytometer analysis of U87 and LN18 glioblastoma cells control samples, treated with different concentrations at different times, did not show modulation in the cell cycle phases at 24, 48, and 72 h (Figure 4), respectively.

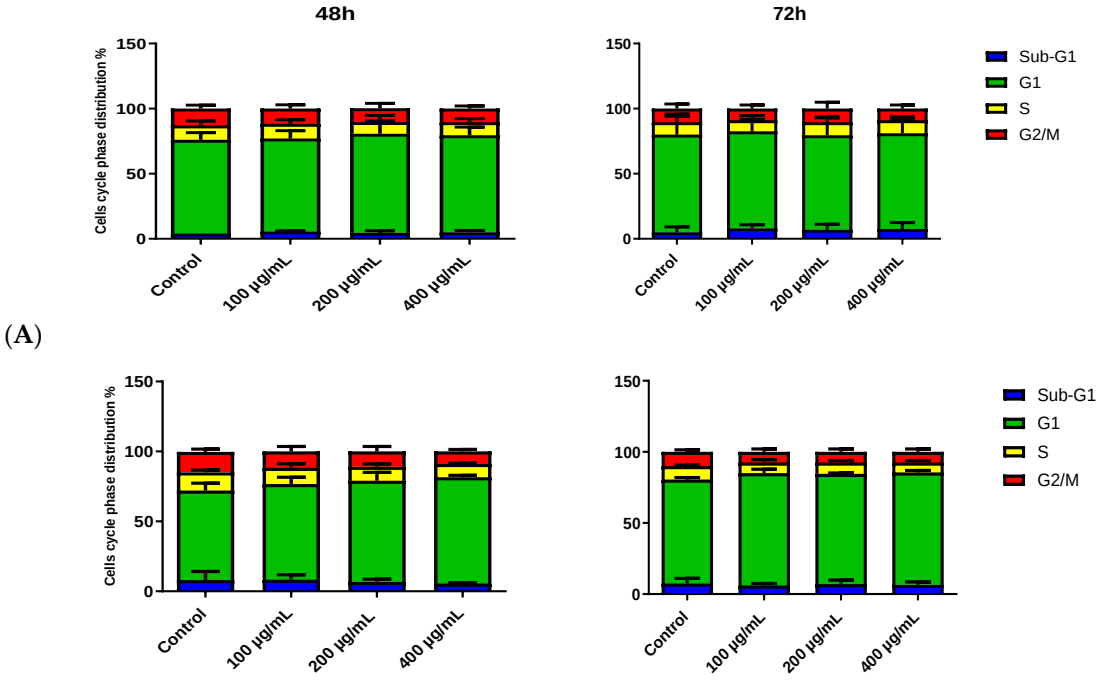

Figure 4. Cell cycle analysis. Percentages of U87 (**A**) and LN18 (**B**) cells in the different phases of the cell cycle after treatment with 100, 200, and 400 µg/mL of peel extract at 48 and 72 h by DNA flow cytometry analysis using Kaluza software for analysis v. 2.2 (Beckman Coulter). Values are the means ± SD of three individual measurements.

3.7. Wound Assay

The chemotherapy failure and the difficulties in glioma treatment are also caused by the cell's ability to infiltrate adjacent healthy tissues [28]. Roooprai et al. [29], studied the anti-invasive activities of four citrus flavonoids, demonstrating that tangeretin and chokeberry extracts can reduce the migration and invasiveness of glioma cells. In order to propose another integrative treatment for glioma, after the previous results demonstrating the absence of *C. australasica* cytotoxicity against U87 and LN18 cancer cells, we have focused attention on the use of peel extract as anti-invasive phytocomplex for glioma management. For this reason, wound-healing experiments were conducted to evaluate the effects of 100, 200, and 400 µg/mL of citrus peel extract on the migration ability of U87 and LN18 cells. Figures 5 and 6 illustrate the wound healing of U87 and LN18 cells, respectively, treated with *C. australasica* peel extract compared to their controls. The results indicate that as the concentration of peel extract increases, the migration ability of U87 cells decreases (85% control vs. 50% at 400 µg/mL), and this effect was even more pronounced in resistant LN18 cells (93% control vs. 15% at 400 µg/mL).

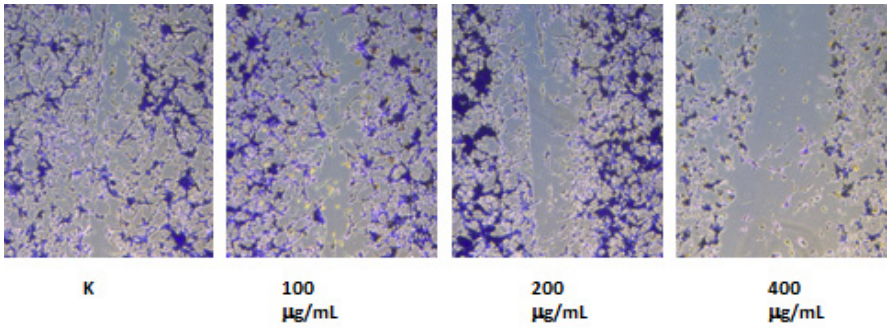

(**A**)

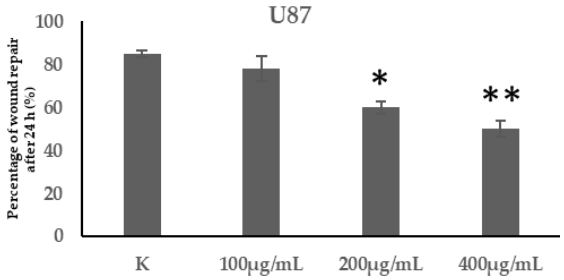

(**B**)

Figure 5. (**A**) Representative wound-healing profiles in U87 cells after *C. australasica* peel extract treatments (Control, 100, 200, and 400 µg/mL, respectively). (**B**) Graphical profile of the migration ability of U87 cells. All experiments were conducted in triplicate and the results are expressed as mean ± SD values. According to GraphPad Prism10, unpaired *t*-test, * *p*-value < 0.05, ** *p*-value < 0.01.

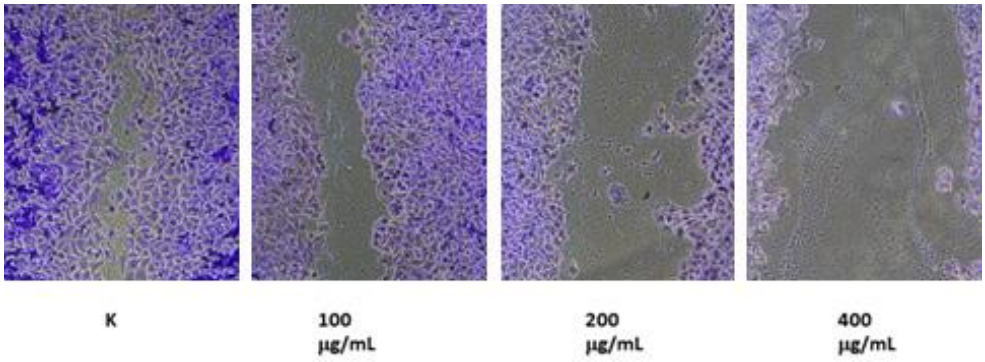

(**A**)

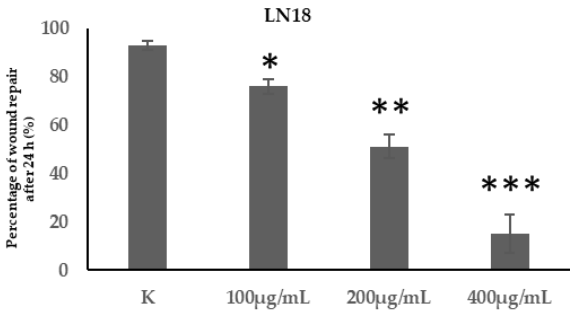

(**B**)

Figure 6. (**A**) Representative wound-healing profiles in LN18 cells after peel extract treatments (Control, 100, 200, and 400 µg/mL, respectively). (**B**) Graphical profile of the migration ability of LN18 cells. All experiments were conducted in triplicate and the results are expressed as mean ± SD values. According to GraphPad Prism10, unpaired *t*-test, * *p*-value < 0.05, ** *p*-value < 0.01, *** *p*-value < 0.001.

3.8. Flow Cytometry (FC) CD44 Evaluation

Given the results obtained from the wound assay, we then evaluated the expression of CD44, which has been implicated in numerous cancer phenotypes, including enhanced cell proliferation, migration, and metastasis [30]. Recently, a meta-analysis study has demonstrated a negative correlation between CD44 expression and GBM patient survival [31,32]. GBM cells expressing CD44 can efficiently colonize and adhere to the extracellular matrix of the tissue environment. In this way, CD44 modulation influences GBM cell proliferation and migration by degrading hyaluronate and disrupting normal brain tissue [33]. These results showed that citrus peel extract reduces CD44 expression on the cell membrane of U87 and LN18 cell lines in terms of mean fluorescence intensity. After treatment with 100, 200, and 400 µg/mL of citrus peel extract at different times, a reduction in CD44 expression level was observed at 400 µg/mL of citrus peel extract after 48 and 72 h in U87 cells, 1.6 and 2.2-fold, while a reduction was observed in LN18 cells after treatment with 400 µg/mL of extract to for 72 h. LN18 cells showed a 1.8-fold decrease in CD44 expression level compared to the control. The results indicated that the treatment for 72 h with 400 µg/mL of citrus peel extract reduced CD44 expression levels in both U87 and LN18 glioblastoma cell lines (Figure 7).

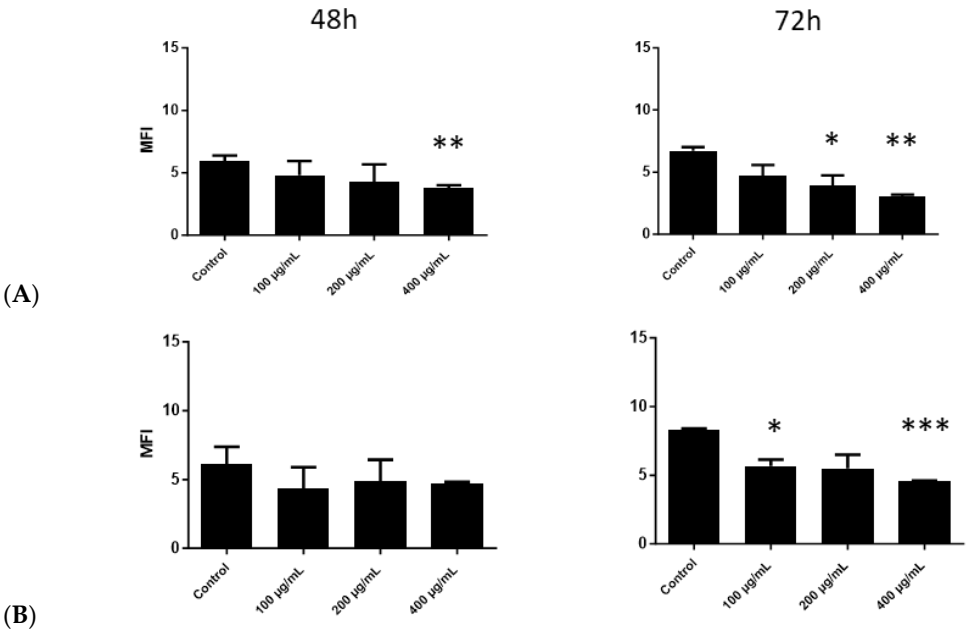

Figure 7. Flow cytometric analysis of CD44 expression. U87 (**A**) and LN18 (**B**) cells after treatment with 100, 200, and 400 µg/mL of peel extract at 48 and 72 h, were stained with Alexa-Fluor 488-conjugated anti-CD44 antibody. Negative controls are cells labeled with secondary goat–anti-mouse IgG Alexa-Fluor 488-conjugate. Flow cytometric analysis was performed as described in the Materials and Methods. Change in mean fluorescence intensity is depicted as mean ± SD of three independent experiments. According to GraphPad Prism10, unpaired *t*-test, * *p*-value < 0.05, ** *p*-value 0.001 to 0.01, *** *p*-value 0.0001 to 0.001.

3.9. CD44 Expression by Immunofluorescence Microscopy on U87 and LN18 Cells

Immunofluorescent microscopy revealed a heterogeneous staining pattern, indicating that CD44 antigens might cluster on the cell surface of control cells. Intense staining was observed in polarized extensions and membrane regions that appearing to extrude from the control U87 cells often localizing to polarized areas of the cell body where actin stress fibers are commonly present (Figure 8A, arrowheads). After 48 h of treatment with 200 µg/mL peel extract (Figure 8B), CD44 proteins were localized on the cell surface. However, cells treated with 400 µg/mL showed a significant reduction in CD44 molecules on their surface (Figure 8C). In LN18 cells treated with 200 and 400 µg/mL of the extract for 48 h, CD44

antigens were generally detected on the cellular membranes without specific localization. Additionally, in Figure 9C, the reduction in CD44 molecules was more pronounced than in Figure 9B, correlating with FACS results. At the same time, in LN18 control cells, CD44 adhesion proteins were mainly detected on the cell body where actin stress fibers are commonly present (Figure 9A, arrowheads).

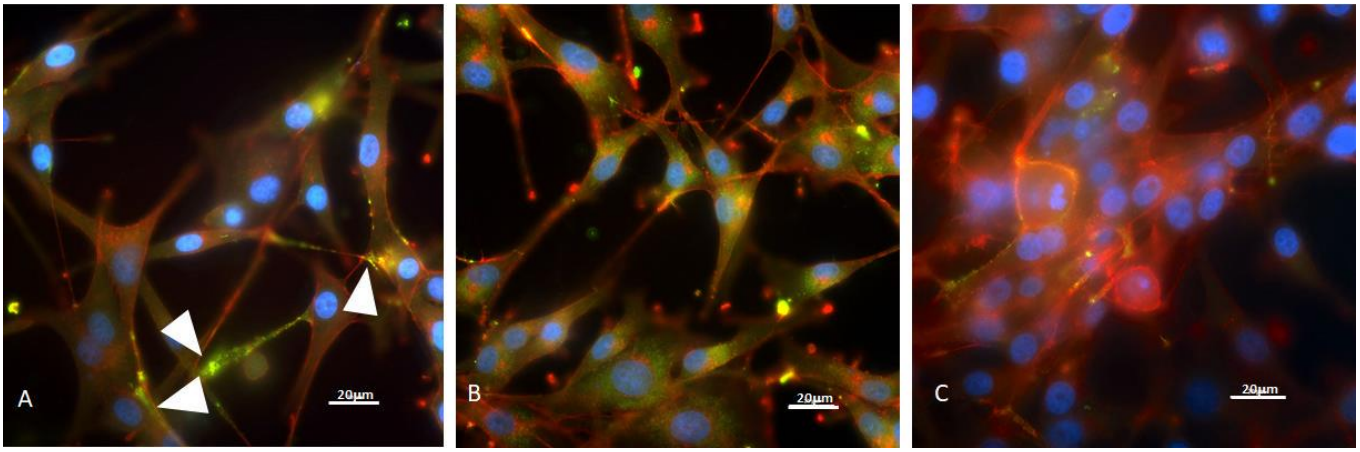

Figure 8. Expression of CD44 molecules on U87 human glioma cells. Immunofluorescence observations on (**A**) (Control), (**B**) (200 µg/mL), and (**C**) (400 µg/mL) of peel extract after 48 h of treatment. Green color indicates CD44 molecule, red color indicates actin filaments stained by Alexa Fluor™ Plus 555 Phalloidin and blue color indicates nuclei stained by Hoechst 33258.

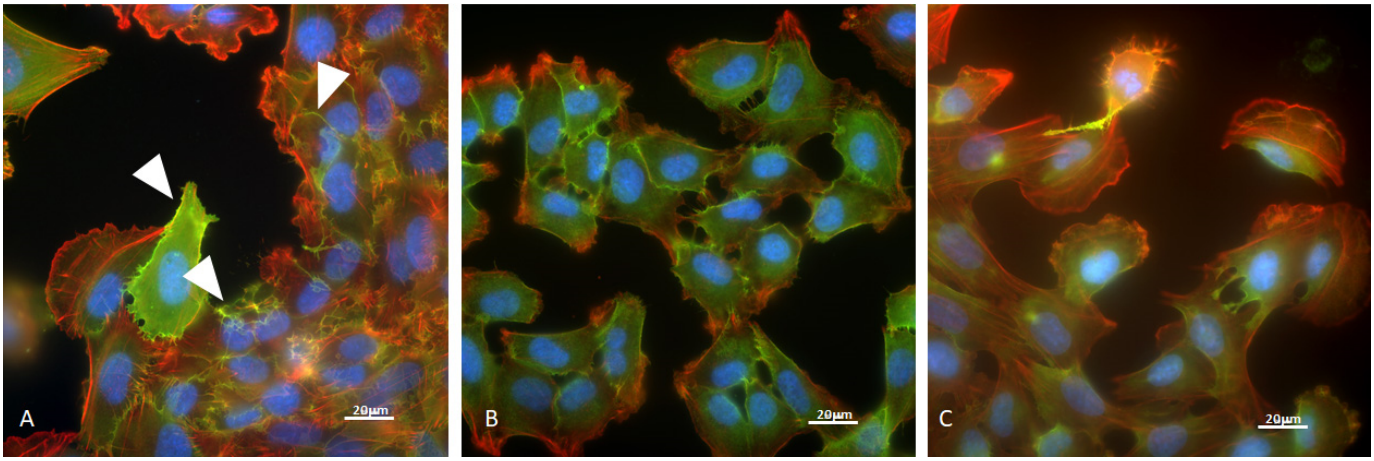

Figure 9. Expression of CD44 molecules on LN18 human glioma cells. Immunofluorescence observations on (**A**) (control), (**B**) (200 µg/mL), and (**C**) (400 µg/mL) of peel extract after 48 h of treatment. Green color indicates CD44 molecule, red color indicates actin filaments stained by Alexa Fluor™ Plus 555 Phalloidin and blue color indicates nuclei stained by Hoechst 33258.

The results of this study reveal a significant relationship between the concentration of citrus peel extract treatments and the migratory behavior of glioma cells. When the concentration of citrus peel extract increases, there is a significant decrease in the ability of tumor cells to migrate and repair wound damage; particularly in the LN18 glioblastoma cell line (Figure 7). These trends are consistent with the results obtained using fluorescence microscopy. This finding suggests that citrus peel extract could potentially serve as an inhibitor of cell migration and, consequently, the development of metastases in brain tissue. Notably, the effect is more pronounced in the LN18 cell line, where there are higher levels of P-glycoprotein (Pgp) compared to the U87 cell line. This observation aligns with previous

research by Colone et al. [34], which demonstrated the involvement of Pgp in migration processes in melanoma cells as well.

Moreover, the major receptor for hyaluronan, CD44, is involved in glioma invasion and is over-expressed in glioblastoma cancer cells [33,35]. The results show that citrus peel extract treatment reduces CD44 expression in glioma cells (U87 and LN18, respectively). This effect could be caused by the disruption or alteration of the signaling pathways associated with migration, potentially explaining the observed decrease in migratory capacity in response to citrus peel extract treatment. These findings suggest a novel therapeutic approach for arresting glioma migration and metastasis through the modulation of cellular pathways influenced by this phytocompound. Further investigations into the molecular mechanisms underlying these effects, particularly concerning Pgp expression and the associated signaling pathways, are warranted to fully elucidate the therapeutic potential of citrus peel extract in glioma management.

4. Conclusions

In this paper, with the aim to chemically characterize *C. australasica*, different analytical techniques were used which highlighted the presence of a high number of volatile and non-volatile compounds, belonging to different chemical classes. To explore the biological potential of this matrix, several activity essays were conducted. The study of the inhibition of ChEs showed that only the citrus peel extract weakly inhibited AChE enzyme. Flow cytometry results showed that the extract was more effective in down-regulating the expression of the adhesion molecule CD44, as confirmed by immunofluorescence analysis. Moreover, wound assay data supported its ability to reduce glioblastoma cell's motility.

In conclusion, the phytochemical screening revealed a different composition for different parts of the fruit with a large pool of identified bioactive compounds. In particular, the obtained results highlighted how the peel, as a by-product of citrus processing, has an important bioactivity. In conclusion, this preliminary study may be relevant for the valorization of residual biomass, considered as waste. Further studies will be necessary to better investigate the composition–activity correlation to reveal the possible mechanisms underlying the biological effects of *C. australasica* peel.

Author Contributions: Conceptualization, D.D.V. and S.G.; methodology, D.D.V., A.R.S., M.C., M.L.D., F.S., L.S. and S.G.; formal analysis, D.D.V., A.R.S., M.C., M.L.D., F.S. and S.G.; investigation, D.D.V., A.R.S., M.C., M.L.D., F.S. and S.G.; resources, S.G.; data curation, D.D.V., A.R.S., M.C., M.L.D., F.S., L.S., S.G.; writing—original draft preparation, D.D.V., A.R.S., M.C., M.L.D., F.S. and S.G.; writing—review and editing, D.D.V., A.R.S., M.C., M.L.D., F.S., L.S. and S.G.; supervision, D.D.V. and S.G.; project administration, S.G. All authors have read and agreed to the published version of the manuscript.

Funding: This research received no external funding.

Institutional Review Board Statement: Not applicable.

Informed Consent Statement: Not applicable.

Data Availability Statement: The original contributions presented in the study are included in the article, further inquiries can be directed to the corresponding author.

Acknowledgments: The authors are thankful to Niels Rodin's citrus farm, Switzerland, for providing *Citrus caviar* species.

Conflicts of Interest: The authors declare no conflicts of interest.

References

1. Wang, X.; Ouyang, Y.; Liu, J.; Zhu, M.; Zhao, G.; Bao, W.; Hu, F.B. Fruit and vegetable consumption and mortality from all causes, cardiovascular disease, and cancer: Systematic review and dose-response meta-analysis of prospective cohort studies. *BMJ* **2014**, *349*, g4490. [CrossRef] [PubMed]
2. Zou, Z.; Xi, W.; Hu, Y.; Nie, C.; Zhou, Z. Antioxidant activity of Citrus fruits. *Food Chem.* **2016**, *196*, 885–896. [CrossRef]

3. Ladaniya, M.S. Nutritive and medicinal value of citrus fruits. In *Citrus Fruit Biology, Technology and Evaluation*; Ladaniya, M.S., Ed.; Academic Press: Cambridge, MA, USA, 2008.
4. Lv, X.; Zhao, S.; Ning, Z.; Zeng, H.; Shu, Y.; Tao, O.; Xiao, C.; Liu, C.; Liu, Y. Citrus fruits as a treasure trove of active natural metabolites that potentially provide benefits for human health. *Chem. Cent. J.* **2015**, *9*, 68. [CrossRef] [PubMed]
5. Lourenço, S.C.; Moldão-Martins, M.; Alves, V.D. Antioxidants of Natural Plant Origins: From Sources to Food Industry Applications. *Molecules* **2019**, *24*, 4132. [CrossRef] [PubMed]
6. Hamilton, K.N.; Ashmore, S.E.; Drew, R.A. Development of conservation strategies for *Citrus* species of importance to Australia. *Acta Hortic.* **2005**, *694*, 111–115. [CrossRef]
7. Delort, E.; Yuan, Y.-M.; Rodrigues, S.; de Oliveira Silva, E.; de Brito, E.S. (Eds.) *Finger lime/the Australian caviar—Citrus australasica*; Exotic Fruits Academic Press: Cambridge, MA, USA, 2018; pp. 203–210.
8. Hawkeswood, T.J. A review of some publications concerning Citrus (*Microcitrus*) *australasica* F. Muell. (Rutaceae) in Australia and South-East Asia (mostly Thailand). *Calodema* **2017**, *581*, 1–14.
9. Adhikari, B.; Dutt, M.; Vashisth, T. Comparative phytochemical analysis of the fruits of four Florida-grown finger lime (*Citrus australasica*) selections. *LWT* **2021**, *135*, 110003. [CrossRef]
10. Vitalini, S.; Iriti, M.; Vinciguerra, V.; Garzoli, S. A Comparative Study of the Chemical Composition by SPME-GC/MS and Antiradical Activity of Less Common *Citrus* Species. *Molecules* **2021**, *26*, 5378. [CrossRef] [PubMed]
11. Vitalini, S.; Iriti, M.; Ovidi, E.; Laghezza Masci, V.; Tiezzi, A.; Garzoli, S. Detection of Volatiles by HS-SPME-GC/MS and Biological Effect Evaluation of Buddha's Hand Fruit. *Molecules* **2022**, *27*, 1666. [CrossRef] [PubMed]
12. Wishart, D.S.; Guo, A.; Oler, E.; Wang, F.; Anjum, A.; Peters, H.; Dizon, R.; Sayeeda, Z.; Tian, S.; Lee, B.L.; et al. HMDB 5.0: The Human Metabolome Database for 2022. *Nucleic Acids Res.* **2022**, *7*, 622–631. [CrossRef]
13. Ellman, G.L.; Courtney, K.D.; Andres, V., Jr.; Featherstone, R.M. A new and rapid colorimetric determination of acetylcholinesterase activity. *Biochem. Pharmacol.* **1961**, *7*, 88–95. [CrossRef]
14. Dhungel, L.; Rowsey, M.E.; Harris, C.; Raucher, D. Synergistic Effects of Temozolomide and Doxorubicin in the Treatment of Glioblastoma Multiforme: Enhancing Efficacy through Combination Therapy. *Molecules* **2024**, *29*, 840. [CrossRef]
15. Towner, R.A.; Smith, N.; Saunders, D.; Brown, C.A.; Cai, X.; Ziegler, J.; Mallory, S.; Dozmorov, M.G.; Coutinho De Souza, P.; Wiley, G.; et al. OKN-007 Increases temozolomide (TMZ) Sensitivity and Suppresses TMZ-Resistant Glioblastoma (GBM) Tumor Growth. *Transl. Onc.* **2019**, *12*, 320–335. [CrossRef]
16. Johnson, J.B.; Batley, R.; Manson, D.; White, S.; Naiker, M. Volatile compounds, phenolic acid profiles and phytochemical content of five Australian finger lime (*Citrus australasica*) cultivars. *LWT* **2022**, *154*, 112640. [CrossRef]
17. Al Juhaimi, F.; Musa Özcan, M.; Uslu, N.; Ghafoor, K.; Babiker, E.E.; Adiamo, O.K.; Alsawmahi, O.N. The effects of conventional heating on phenolic compounds and antioxidant activities of olive leaves. *J. Food Sci. Technol.* **2018**, *55*, 4204–4211. [CrossRef]
18. Al Juhaimi, F.; Özcan, M.M.; Uslu, N.; Ghafoor, K. The effect of drying temperatures on antioxidant activity, phenolic compounds, fatty acid composition and tocopherol contents in citrus seed and oils. *J. Food Sci. Technol.* **2018**, *55*, 190–197. [CrossRef]
19. Reazai, M.; Mohammadpourfard, I.; Nazmara, S.; Jahanbakhsh, M.; Shiri, L. Physicochemical Characteristics of Citrus Seed Oils from Kerman, Iran. *J. Lipids* **2014**, *1*, 174954. [CrossRef]
20. Tan, T.; Li, J.; Luo, R.; Wang, R.; Yin, L.; Liu, M.; Zeng, Y.; Zeng, Z.; Xie, T. Recent Advances in Understanding the Mechanisms of Elemene in Reversing Drug Resistance in Tumor Cells: A Review. *Molecules* **2021**, *26*, 5792. [CrossRef]
21. Aznar, R.; Rodríguez-Pérez, C.; Rai, D.K. Comprehensive Characterization and Quantification of Antioxidant Compounds in Finger Lime (*Citrus australasica* L.) by HPLC-QTof-MS and UPLC-MS/MS. *Appl. Sci.* **2022**, *12*, 1712. [CrossRef]
22. Abdel-Salam, O.M.; Youness, E.R.; Mohammed, N.A.; Morsy, S.M.; Omara, E.A.; Sleem, A. Citric acid effects on brain and liver oxidative stress in lipopolysaccharide-treated mice. *J. Med. Food* **2014**, *17*, 588–598. [CrossRef] [PubMed]
23. Niaz, K.; Nawaz, M.A.; Pervez, S.; Younas, U.; Shah, I.; Khan, F. Total scale analysis of organic acids and their role to mitigate Alzheimer's. *S. Afr. J. Bot.* **2022**, *144*, 437–447. [CrossRef]
24. Sadaoui, N.; Bec, N.; Barragan-Montero, V.; Kadri, N.; Cuisinier, F.; Larroque, C.; Ara, K.; Khettal, B. The essential oil of Algerian *Ammodaucus leucotrichus* Coss. & Dur. and its effect on the cholinesterase and monoamine oxidase activities. *Fitoterapia* **2018**, *130*, 1–5.
25. Baset, M.A.; Islam, M.S.; Shamsuddin, Z.H. Altered sex expression by plant growth regulators: An overview in medicinal vegetable bitter gourd (*Momordica charantia* L.). *J. Med. Plants Res.* **2014**, *8*, 361–367.
26. Olennikov, D.N.; Kashchenko, N.I.; Chirikova, N.K.; Akobirshoeva, A.; Zilfikarov, I.N.; Vennos, C. Isorhamnetin and Quercetin Derivatives as Anti-Acetylcholinesterase Principles of Marigold (*Calendula officinalis*) Flowers and Preparations. *Int. J. Mol. Sci.* **2017**, *18*, 1685. [CrossRef]
27. Chung, Y.-K.; Heo, H.-J.; Kim, E.-K.; Kim, H.-K.; Huh, T.-L.; Lim, Y.; Kim, S.-K.; Shin, D.-H. Inhibitory Effect of Ursolic Acid Purified from *Origanum majorana* L. on the Acetylcholinesterase. *Mol. Cells* **2011**, *2*, 137–143. [CrossRef]
28. Da Ros, M.; De Gregorio, V.; Iorio, A.L.; Giunti, L.; Guidi, M.; de Martino, M.; Genitori, L.; Sardi, I. Glioblastoma chemoresistance: The double play by microenvironment and blood-brain barrier. *Int. J. Mol. Sci.* **2018**, *19*, 2879. [CrossRef]
29. Rooprai, H.K.; Christidou, M.; Murray, S.A.; Davies, D.; Selway, R.; Gullan, R.W.; Pilkington, G.J. Inhibition of Invasion by Polyphenols from Citrus Fruit and Berries in Human Malignant Glioma Cells In Vitro. *Anticancer Res.* **2021**, *41*, 619–633. [CrossRef]
30. Zöller, M. CD44: Can a Cancer-Initiating Cell Profit from an Abundantly Expressed Molecule? *Nat. Rev. Cancer* **2011**, *11*, 254–267. [CrossRef]

31. Si, D.; Yin, F.; Peng, J.; Zhang, G. High Expression of CD44 Predicts a Poor Prognosis in Glioblastomas. *Cancer Manag. Res.* **2020**, *12*, 769–775. [CrossRef]
32. Hou, C.; Lin, H.; Wang, P.; Yang, Y.; Cen, S.; Zhou, D. Comment on "Expression of CD44 and the Survival in Glioma: A Meta-Analysis". *Biosci. Rep.* **2020**, *40*, BSR20202812. [CrossRef]
33. Mishra, M.N.; Chandavarkar, V.; Sharma, R.; Bhargava, D. Structure, Function and Role of CD44 in Neoplasia. *J. Oral Maxillofac. Pathol.* **2019**, *23*, 267–272. [CrossRef] [PubMed]
34. Colone, M.; Calcabrini, A.; Toccacieli, L.; Bozzuto, G.; Stringaro, A.; Gentile, M.; Cianfriglia, M.; Ciervo, A.; Caraglia, M.; Budillon, A.; et al. The Multidrug Transporter P-Glycoprotein: A Mediator of Melanoma Invasion? *J. Investig. Dermatol.* **2008**, *128*, 957–971. [CrossRef] [PubMed]
35. Inoue, A.; Ohnishi, T.; Nishikawa, M.; Ohtsuka, Y.; Kusakabe, K.; Yano, H.; Tanaka, J.; Kunieda, T. A Narrative Review on CD44′s Role in Glioblastoma Invasion, Proliferation, and Tumor Recurrence. *Cancers* **2023**, *15*, 4898. [CrossRef] [PubMed]